Compressive properties of nano-particle modified epoxy resin at different strain rates

T. Gómez-del Río, J. Rodríguez, R.A. Pearson

PII: S1359-8368(13)00567-2
DOI: http://dx.doi.org/10.1016/j.compositesb.2013.10.002
Reference: JCOMB 2679

To appear in: *Composites: Part B*

Received Date: 24 June 2013
Revised Date: 2 September 2013
Accepted Date: 2 October 2013

Please cite this article as: Gómez-del Río, T., Rodríguez, J., Pearson, R.A., Compressive properties of nano-particle modified epoxy resin at different strain rates, *Composites: Part B* (2013), doi: http://dx.doi.org/10.1016/j.compositesb.2013.10.002

Compressive properties of nano-particle modified epoxy resin at different strain rates

T. Gómez-del Río*[1], J. Rodríguez[1] and R.A. Pearson[2]

[1]DIMME. Departamento de Tecnología Mecánica. ESCET. Universidad Rey Juan Carlos.
c/Tulipán s/n, Móstoles (Madrid), Spain.

[2]Center for Polymer Science and Engineering, Lehigh University, 5 East Packer Avenue,
Bethlehem, PA 18015, USA.

ABSTRACT

Epoxy resins often exhibit high strength yet are often brittle, especially at high strain rates. Block copolymer modified epoxy resins have generated significant interest since it was demonstrated that the combination could lead to nanostructured thermosets through the self-assembly of the block copolymer. Such nanostructured epoxies exhibit increased ductility without the significant loss in yield strength exhibited by traditional rubber-modified epoxies. In this study, the effect of different nanoscale additives on the compressive yield strength of a model epoxy resin has been studied. In the first case, a block copolymer styrene-b-butadiene-b-polymethylmethacrylate (SBM) was added to the model epoxy resin. In the second case, carbon nantubes (CNTs) were added. In the final case, both additives were mixed simultaneously with the epoxy resin. The compressive mechanical behaviour of these materials has been investigated over a wide range of strain rates (0.001 to 3500 s^{-1}). The yield behaviour was found to fit the cooperative yield model proposed by Fotherigham and Cherry.

---

*Corresponding author: Telephone: +34 914887176, e-mail: mariateresa.gomez@urjc.es

KEYWORDS

A. Polymer-matrix composites. A. Nano particle. B. Mechanical properties. Yielding.

1. INTRODUCTION

Epoxy resins are preferred as matrices for high performance structural composite materials and other industrial applications, such as protective coatings, adhesives, electrical insulation, due to their good mechanical strength and easy processability. Unfortunately, the same crosslinked structure that imparts high stiffness, strength and use temperature results in poor fracture resistance. Fortunately, it is well known that incorporation of rubber particles, rigid fillers or thermoplastic resins can effectively improve the toughness of lightly epoxy resin systems [1-14]. However, addition of rubber particles in epoxy systems decreases stiffness and strength when compared to pure epoxies or epoxies reinforced with rigid agents [7-14]. Incorporation of rigid particle fillers, such as silica, and alumina can improve the toughness of epoxy resins without substantial reduction in the glass transition temperature. However, in comparison with rubber-modified epoxy, the improvement in toughness is much lower.

Soft particles and rigid fillers can be simultaneously added into an epoxy resin enhancing mechanical properties as well as toughness. Such materials are often referred to as hybrid particulate composites and there are several examples in the literature that suggest synergistic interactions in such systems can provide more fracture toughness than either type of particle alone [15-17]. Practically speaking, reinforcing particles are added to rubber-toughened blends to compensate for the decrease in stiffness and strength due the presence of the soft particles.

Recently, significant work has been conducted examining the utility of nanometer size rubber particles to improve the mechanical and thermal performance of epoxy resins [18-23]. Both diblock and triblock copolymers can naturally self-assemble into hierarchical substructures at the nanometer scale. Such substructures include vesicles, spherical micelles, and worm-like micelles. Some researchers believe that vesicle formation is the optimal morphology for toughening purposes [20]. Triblock copolymers such as SBM (polystyrene-block-polybutadiene-block-poly(methyl methacrylate)) can form additional types of nanoscale microstructures in epoxy resins [21]. Significant improvements in toughness have been observed with these nanosize morphologies [24]. Indeed, SBM copolymers are readily soluble in many noncured epoxy-amine mixtures; however, maintaining compatibility throughout the whole curing process is critical to maintaining the nanostructured blends. Fortunately, SBM can be modified with reactive groups to overcome compatibility issues in some epoxy systems[23].

This work examines the use of a commercial triblock copolymer of SBM from Arkema with a DGEBA epoxy matrix and also with carbon nanotubes as reinforcement. Carbon nanotubes (CNTs) have emerged as potential candidates for modification of an epoxy matrix because of their exceptional strength and stiffness, high flexibility and elongation at break, and high thermal and electrical conductivity. The resulting morphology of these systems and their mechanical behavior under compression loading at different strain rates will be discussed in this paper.

2. EXPERIMENTAL

2.1. Materials

For this study a diglycidylether of bisphenol A (DGEBA–DER 331 epoxy resin from the Dow Chemical, CO) with an epoxy equivalent weight of 187 g/equiv was cured with an amine-based curing agent, piperidine. The piperidine was added to the epoxy at a concentration of 5 parts per hundred parts resin (phr). One styrene/butadiene/methacrylate (SBM) triblock copolymer commercially designated, by Arkema as Nanostrength^{TM} E21, was used as the soft toughening agent. This novel toughening agent was studied at a loading level of 5 phr. The commercial triblock copolymer used as toughening agent developed to self-assemble on the nanoscale level hence providing nanosize toughening phases. Nanocomposites were formulated by diluting the carbon nanotubes concentrate (Nanosolve^{TM}) with neat epoxy resin to produce epoxies with 0.25 phr concentrations of CNTs. For all the materials, the final mixture was thermally cured at 160ºC for 6h.

2.2. Microscopy chracterization

In order to observe the phase structure of epoxy systems, the samples were fractured under cryogenic condition immersed in liquid nitrogen. The fractured surfaces so obtained were coated with thin layers of platinum of about 100 Å to improve the electrical conductivity that reduces charge build-up on the surface. All specimens were examined with an Nanosem 230 Field emission scanning electron microscope (FE-SEM) with acceleration voltage between 3 and 5 kV.

Also transmission electron microscopy (TEM) was performed using a Philips Tecnai 20 field emission gun transmission electron microscope with aceleration voltage of 200kV. Thin sections (40 nm) were cut from the samples at -90 ºC using a Leica EMFC6 ultramicrotome with a diamond knife. The sections were stained using Ruthenium tetraoxide (RuO_4) vapor to increase the contrast. The stained specimen sections were placed in mesh copper grids for observation.

2.3. Mechanical characterization

Quasi-static compression tests were performed using an electromechanical MTS universal testing machine with a load frame of 100kN. Samples were tested at three different engineering strain rates ranging from 0.001 to 0.1s^{-1}. Cylindrical specimens were machined with dimensions of 6mm in thickness and 5.5mm in diameter. To minimise interfacial friction the specimen surfaces contacting the polished metal surfaces were lubricated with CastrolTM LMX grease. At least three specimens were tested for each strain rate, allowing evaluation of the test reproducibility and to obtain an average value.

In order to measure the strain in the specimen during the test, a LIMESS video-extensometer was and a commercial Vic2D digital image correlation (DIC) system was used to measure the displacement field during loading. The image correlation technique needs a textured object, so the surfaces of the specimens were marked with a random pattern of spray paint. The DIC technique gives the displacement field. The strain field is computed by numerical derivation of the displacement field.

Dynamic compression tests were conducted using a split Hopkinson pressure bar (SHPB). The SPHB device basically consists of an input bar, an output bar and a small cylindrical specimen located between them. Both bars are made of a high yield strength steel, 20mm in diameter and lengths of 1.2 and 0.8m for the input and output bars, respectively (Fig. 1). The projectile, a bar of approximately 0.3m in length, is impelled against the input bar by means of an air gun. Due to the impact, an elastic compression pulse is generated in the input bar and travels along it up to the specimen, where is partially reflected and partially transmitted to the output bar. The amount of reflected and transmitted wave depends on the impedance difference of the bars and the specimen. In the case of the steel bars, the impedance is much higher than in the case of the polymer specimen. Nevertheless, for these samples, the transmitted wave has been good enough to measure it and assure the equilibrium in the specimen. To measure the incident, reflected and transmitted pulses, strain gauges (VISHAY J2A-06-S047K-350) are attached to the bars. The strain gauge signals are recorded using a VISHAY 2200 conditioner connected to a TEKTRONIX TDS 420A digital oscilloscope. In the input bar two gauge system was used in order to work with longer incident waves.

The length to diameter ratio, *l/d*, of the specimens must be carefully chosen to ensure that stress equilibrium is achieved during the whole test. This equilibrium is achieved after an initial period which has to be as short as possible but it is dependent on the wave velocity within the specimen. Many researchers agree that this stress equilibrium requires approximately four wave reverberations in the specimen. One solution is to reduce the thickness of the specimen which reduces the propagation time. So, the specimen height should not be as high as that of quasi-static tests. Due to the size of the microstructure of the materials studied, small specimens can be representative of the massive material. Finally, a thickness of 2.5mm and a diameter of 5.5mm were chosen.

Some high strain rate size specimens (2.5mm length) were tested in quasi-static conditions in order to verify that there was no effect of the specimen height, nevertheless frictional effects were minimized using lubricants at bars, compression plates and specimen interfaces. Results obtained at low strain rates with specimens of both 2.5 and 6mm were similar, so no size effect was observed, at least in the range of lengths.

3. Results and discussion

The morphologies of the thermosets were investigated by transmission electronic microscopy (TEM) and field emission scanning electron microscopy (FE-SEM). The TEM images of the epoxy systems containing 5 phr of SBM triblock copolymer, 0.25 phr CNTs and a mixture of 5 phr SBM and 0.25 phr CNTs are presented in Fig. 2, the thin sections were stained with RuO_4 during 15 or 20 minutes in order to provide contrast in the micrographs.

The TEM observations indeed indicate that the nanostructured epoxy thermosets were obtained. A dispersed phase morphology at the nanometer scale was observed in all the cases. The dark objects are assigned to SBM phases since the triblock copolymer domains containing C-C double bonds can be preferentially stained with RuO_4. The spherical SBM phases were homogenously dispersed in the continuous epoxy matrix with an average size of 60±12 nm. It is seen that the size of the SBM nanoparticles increases when adding at the same time the carbon nanotubes, in this latest case, the average size of the particles is 88±20 nm, but the morphology of the hybrid composites is quite similar to the epoxy SBM modified.

The SBM phase observed can be interpreted as a spherical , core-shell morphology, and as it is usually observed for this SBM triblock copolymers [25], with a heavily stained (black) PB shell and a lightly stained (gray) PS core. The PMMA block is difficult to observe in these systems.

In the CNTs reinforced epoxy and hybrid compounds good dispersion of the nanotubes is observed with random orientation. Nevertheless, the nanotubes did not appear straight and tend to coil. The waviness of the carbon nanotubes has a clear effect in the effective mechanical properties of the composite, decreasing these properties when compared to the straight nanotubes assumption [26].

The morphology of the epoxy systems were also studied by means of field emission scanning electron microscopy (FE-SEM). The FE-SEM micrographs are shown in Fig. 3. The specimens for the morphological observation were prepared via fracturing samples of the materials under cryogenic conditions using liquid nitrogen. The FE-SEM shows the materials displayed the same heterogeneous morphology as observed in the TEM. For the epoxy containing the modifier SBM triblock copolymer, the spherical particles were uniformed dispersed in the continuous matrix, however the average size of the voids generated during the fracture process is a bit higher than the particle size measured by TEM, indicating that even the fracture process has been performed at very low temperatures, some matrix dilation has taken place.

Fig. 4 shows the stress-strain curves of neat epoxy resin (top) and its corresponding nanocomposites (bottom) at various strain rates. According to these results, pure epoxy resin, CNTs reinforced composite and SBM rubber modified epoxy are very sensitive to strain rate as expected.

All curves present a similar aspect: after the initial linear region, a significant non-linear region, a maximum corresponding to shear yielding is observed before a subsequent plastic flow process. A decrease in the stress after yielding indicates strain softening, which is commonly observed in ductile amorphous polymers. Strain softening is follow by plastic flow and then a marked strain hardening in all cases. The yield point is defined in the same way for both low and high strain rates, and it is the maximum of the stress–strain curve before the softening. As expected, yield strength and flow stress of all the materials tested significantly increase with increasing strain rate whereas the modulus shows a relatively modest increase. The dependence of the compressive yield strength on strain rate is shown for the four different materials in Fig. 5.

The strain softening is caused by the formation of shear bands. The location of shear deformation causes the volume strain to exhibit a maximum. This maximum occurs at increasingly high strains as the strain rate increases. The retardation of the shear localization process by increasing strain rates is undoubtedly an important factor in the brittleness of the neat resins in crack propagation. While the shear localization process is retarded, the volume strain increases. The bulk strain energy increases roughly as the square of the volume strain, so the inability of the shear localization process to take place exacts a penalty in the building up of the bulk energy. Thus, any mechanism that facilitates the shear localization process, or, alternatively, dissipates the bulk strain energy, would enhance the toughness. The rubber particles appear to do both [4]. Yee and Pearson [4-5] showed that at sufficient high strain rates, however, when the neat resins tipically dilate at a nearly constant rate almost up to the yield point, the rubber particles cause the material to expand to a higher rate than the neat epoxy. They presented that this expansion was caused by cavitation of the rubber particles. the cavitation is followed by the onset of the shear process, which would not have taken place in the neat epoxy under the same conditions. Thus, the rubber particles dissipate the bulk strain energy by cavitation, and, at the same time, the shear strain energy is allowed to build up to the point where the shear yielding takes place. The voids left behind by the rubber particles act further as stress concentrators.

The yield behaviour of polymers is normally considered as thermally activated process incorporating strain rate effect. There are several models that predict this behaviour for thermosets polymers and are described elsewhere [27]. As depicted in Fig. 5, the yield stress of the four materials tend to increase in a linear way at low strain rates but there is a significant increase in slope (i.e. rate sensitivity) at high strain rates. The increase in rate sensitivity is associated, with a further reduction in molecular mobility of the polymer chains due to secondary relaxation processes.

Fotherigham and Cherry [28] modified the original Eyring equation raising the hyperbolic sine function to the nth power (where *n* was proposed to be the number of segments participating in the process) and including an internal stress as a new structural parameter, σ_i. The yield behaviuor of pure epoxy resin has been previously successfully described by this cooperative model for yield stress [27]:

$$\sigma_y = \sigma_i + \frac{2kT}{V^*} sinh^{-1} \left(\frac{\dot{\varepsilon}}{\dot{\varepsilon}^*}\right)^{\frac{1}{n}} \qquad (1)$$

where σ_y is the yield stress, T is the absolute temperature, k the Boltzmann's constant, V an activation volume and $\dot{\varepsilon}^*$ a characteristic strain rate.

Fig. 5 shows the curve fit of neat epoxy and the three composites under study. The predicted results are compared to our experimental data. The cooperative model proposed by Fotherigham and Cherry provides predictions of the yield stress that are in good agreement with the experimental data. The parameters used in this cooperative model obtained from the curves for the four materials are given in Table 1. Values of number of segments, *n*, increases for the modified epoxy and composites, and could be due to the decrease in free space to move each polymer chain because of the presence of additives, so more segments are needed to reach the yield point. Another important parameter is the internal stress, σ_i, that decreases for all the composites compared to neat epoxy even thought the yield stress increases for the CNTs reinforced epoxy at room temperature.

A slight increase in yield stress is observed for the carbon nanotubes reinforced epoxies at low strain rates, although the increase at high strain rates is more appreciable. So overall, the addition of CNTs increases the yield stress of the composites compared to pure epoxy. On the other hand, a decrease in yield stress is observed when SBM triblock copolymer is added. This result is expected since the SBM triblock copolymer self assembles into soft spherical particles. Nevertheless, when both kind of particles are added simultaneously, the elastic properties and the yield stress of the hybrid composite are higher than the pure epoxy. This means that, even with the presence of rubber particles, the co-addition of CNTs improves both the yield stress and the toughness of the pure epoxy at the same time.

Moloney et al. [29] developed a model to predict the yield stress of particulate filled epoxies as a function of filler volume fraction. It is used in this paper, even it refers to particle reinforced composites, because it was developed for compression yield behaviour and it is very easy to use as it needs very few data. In Moloney's model, the yield strength was related to the volume fraction of filler as follows:

$$\sigma_{yc} = \frac{\sigma_{ym}}{1-1,2\varphi_f^{2/3}} \qquad (2)$$

where σ_{yc} and σ_{ym} are the yield strengths of the composite and the neat epoxy, respectively and φ_f is the volume fraction of filler. The difference between the model predictions and the different behavior at extreme loading rates may be attributed to a weak interface, because at impact velocities the load transfer is faster between epoxy and reinforcement and this model does not evaluate the effect of the interfacial strength.

In SBM-epoxy systems, a decrease is expected as the disperse particles is a rubber phase. In addition, the experimental results of compressive testing on rubber-modified epoxies are compared with the predicted values based on Lazzeri and Bucknall's model [30]:

$$\sigma_{yr} = \sigma_{ym}\left(1 - 1{,}375\varphi_f\right) \qquad (3)$$

where σ_{yr} and σ_{ym} are the yield stresses of the rubber-modified and neat polymer, respectively and φ_f is the volume fraction of the dispersed phase. This equation was derived by Lazzeri and Bucknall [25] from the experimental data on yield behavior of rubber-modified poly(methyl methacrylate) under uniaxial compression. In general, the Lazzeri and Bucknall's model gives a relatively good estimation on the effect of core–shell particles content on yield strength in the rubber-modified epoxy systems in this study (Fig. 6).

The predicted drop in yield stress with increasing rubber content from Lazzeri and Bucknall's model matches well with experimentally determined values at low contents of core–shell particles as in our case with 5phr of SBM.

In hybrid systems, the compressive yield strength is similar to the value for the epoxy modified by 5phr core–shell rubber particles alone, i.e. the yield strength did not change significantly at low strain rates, nevertheless there is an appreciable increase in impact resistance at high strain rates compared to the rubber modified epoxy, but in general is quite similar to the neat epoxy.

Usually, strain rate sensitivity is presented in terms of stress–strain curves, which show the effect of strain rates on the proportion of materials, such as Young's modulus, strength, flow stress. In reality it should be useful to have a value of strain rate sensitivity, in order to compare different dependences on strain rate. Consequently, further investigation was carried out to quantify the strain rate sensitivity of the epoxy resin in different strain rates ranges. The calculation of strain rate sensitivity was based on the definition of strain rate sensitivity, which can be expressed as follows [27],

$$\beta = \frac{\sigma_2 - \sigma_1}{\ln\left(\frac{\dot{\varepsilon}_2}{\dot{\varepsilon}_1}\right)} \qquad \begin{matrix} \dot{\varepsilon}_2 > \dot{\varepsilon}_1 \\ \varepsilon = 0{,}025 \end{matrix} \qquad (4)$$

where σ_1 and σ_2 is the flow stress at the fixed strain (in this case, the strain used is 0.025) under different strain rates, and $\dot{\varepsilon}_2 > \dot{\varepsilon}_1$.

From Table 2, the strain rate sensitivity of all epoxy systems studied increased as the range of strain rate increased. It is important to note that the addition of particles of SBM and CNTs in the neat epoxy increases the strain sensitivity, which is important for some applications. In addition, SBM modified epoxy had recorded the highest level of strain rate sensitivity in quasi-static region as compared to other materials. However, at dynamic region, CNTs reinforced epoxy displayed the highest strain rate sensitivity.

4. Summary and conclusions

The influence of addition different kind of nanoparticles in epoxy resin system has been studied: SBM triblock copolymer (as rubber nanoparticles), CNTs (as rigid nanofillers) and both kind of particles simultaneously. Compressive behaviour at different strain rates of the materials has been analyzed. The results of this study may be summarized as follows:

1. Addition of carbon nanotubes increases compressive yield strength modestly at low strain rates, but there is a significant increase at high strain rates.
2. Addition of SBM particles decreases the compressive yield strength at both low and high strain rates.
3. Simultaneous addition of both carbon nanotubes and SBM particles modifiers improves the compressive strength compared to the rubber modified epoxy, obtaining similar properties of neat epoxy.
4. The yield behaviour of the four epoxies studied has been compared to some models for compressive yield stress of composites with reasonable success.

Acknowledgments

Authors are indebted to Universidad Rey Juan Carlos, Comunidad de Madrid and Ministerio de Educación of Spain for their financial support through Projects CCG10-URJC/MAT-5413 and MAT2012-37762.

References:

1. Kinloch AJ, Shaw SJ, Tod DA, Hunston DL. Deformation and fracture-behavior of a rubber-toughened epoxy.1. Microstructure and fracture studies. Polymer 1983;24:1341-54.
2. Huang Y, Kinloch AJ. Modeling of the toughening mechanisms in rubber-modified epoxy polymers .1. Finite-element analysis studies. J Mater Sci 1992;27:2753-62.
3. Huang Y, Kinloch AJ. Modeling of the toughening mechanisms in rubber-modified epoxy polymers .2. A quantitative description of the microstructure fracture property relationships. J Mater Sci 1992;27:2763-9.
4. Yee AF, Pearson RA. Toughening Mechanism in Elastomer-Modified Epoxy Resins - Mechanical Studies. J Mater Sci 1986;21:2462-74.
5. Pearson RA, Yee AF. Toughening Mechanism in Elastomer-Modified Epoxy Resins - Microscopy Studies. J Mater Sci 1986;21:2475-88.
6. Pearson RA, Yee AF. The Influence of Particle Size Distribution on the Toughening Mechanisms in Rubber-Modified Epoxy. J Mater Sci 1991;26:3828-44.
7. Lange FF. The interaction of a crack front with a second-phase dispersion. Phil Mag 1970;22:983-92.
8. Rose LRF. Toughening due to crack-front interaction with a second-phase dispersion. Mech Mater 1987;6:11-5.
9. Faber KT, Evans AG. Crack Deflection Processes — I. Theory. Acta Metall 1983;31(4):565-77.

10. Faber KT, Evans AG. Crack Deflection Processes — II. Experiment. Acta Metall 1983;31(4):577-84.
11. Evans AG, Williams S, Beaumont PWR. On the toughness of particulate filled polymers. J Mater Sci 1985;20:3668-72.
12. Lee J, Yee AF. Inorganic particle toughening I: micro-mechanical deformations in the fracture of glass bead filled epoxies Polymer 2001;42:577-88.
13. Lee J, Yee AF. Inorganic particle toughening II: toughening mechanisms of glass bead filled epoxies. Polymer 2001;42:589-97.
14. Pearson RA, Yee AF. The preparation and morphology of PPO-epoxy blends. J Appl Polym Sci 1993;48:1051-60.
15. Tang LC, Zhang H, Sprenger S, Ye L, Zhang Z. Fracture mechanisms of epoxy-based ternary composites filled with rigid-soft particles. Compos Sci Tech 2012; 72(5):558-65.
16. Liang YL, Pearson RA. The toughening mechanism in hybrid epoxy-silica-rubber nanocomposites (HESRNs). . Polymer 2010; 51 (21):4880-90.
17. Liu HY, Wang GT, Mai YW, Zeng Y. On fracture toughness of nano-particle modified epoxy. Compos B: Eng 2011; 42(8): 2170-75.
18. Grubbs RB; Dean JM; Broz ME; Bates FS. Reactive Block Copolymers for Modification of Thermosetting Epoxy Resins. Macromolecules 2000;33:9522-34.
19. Dean JM, Lipic PM, Grubbs RB, Cook RF, Bates FS. Micellar Structure and Mechanical Properties of Block Copolymer-modified Epoxies. J Polym Sci Part B: Polym Phys 2001;39:2996-3010.
20. Dean JM, Grubbs RB, Saad W, Cook RF, Bates FS. Mechanical Properties of Block Copolymer Vesicle and Micelle Modified Epoxies. J Polym Sci Part B: Polym. Phys 2003;41:2444-56.

21. Ritzenthaler S; Court F; David L; Girard-Reydet E; Leibler L; Pascault JP. ABC Triblock Copolymers/Epoxy-Diamine Blends. 1. Keys To Achieve Nanostructured Thermosets. Macromolecules 2002;35:6245-54.
22. Rebizant V, Abetz V, Tournilhac F, Court F, Leibler L. Reactive Tetrablock Copolymers Containing Glycidyl Methacrylate. Synthesis and Morphology Control in Epoxy−Amine Networks. Macromolecules 2003;36:9889-96.
23. Rebizant V, Venet AS, Tournilhac F; Girard-Reydet E, Navarro C, Pascault JP, Leibler L. Chemistry and Mechanical Properties of Epoxy-Based Thermosets Reinforced by Reactive and Nonreactive SBMX Block Copolymers. Macromolecules 2004;37:8017-27.
24. Gómez-del Río T, Salazar A, Rodríguez J, Pearson R. Tenacidad de fractura de resinas epoxi nanoestructuradas. Anales de mecánica de la Fractura 2013; 1:131-5.
25. Périé T, Brosse AC, Tencé-Girault S, Leibler L. Nanostructured films and composites from carbon nanotubes dispersed by ABC block terpolymers in selective solvent. Polymer 2011;52:3065-73.
26. Gómez-del Río T, Poza P, Rodríguez J, García-Gutiérrez MC, Hernández JJ, Ezquerra TA. Influence of single-walled carbon nanotubes on the effective elastic constants of poly(ethylene terephthalate). Compos Sci Tech 2010; 70(2):284-90.
27. Gómez-del Río T, Rodríguez J. Compression yielding of epoxy: Strain rate and temperature effect. Mater Des 2012;35:369-73.
28. Fotheringham D, Cherry BW. The role of recovery forces in the deformation of linear polyethylene. J Mater Sci 1978;13:951–64.
29. Moloney AC, Kausch HH, Kaiser T, Beer HR. Parameters determining the strength and toughness of particulate filled epoxide resins. J Mater Sci 1987;22:381–93.

30. Lazzeri A, Bucknall CB. Applications of a dilatational yielding model to rubber-toughened polymers. Polymer 1995;36:2895–902.

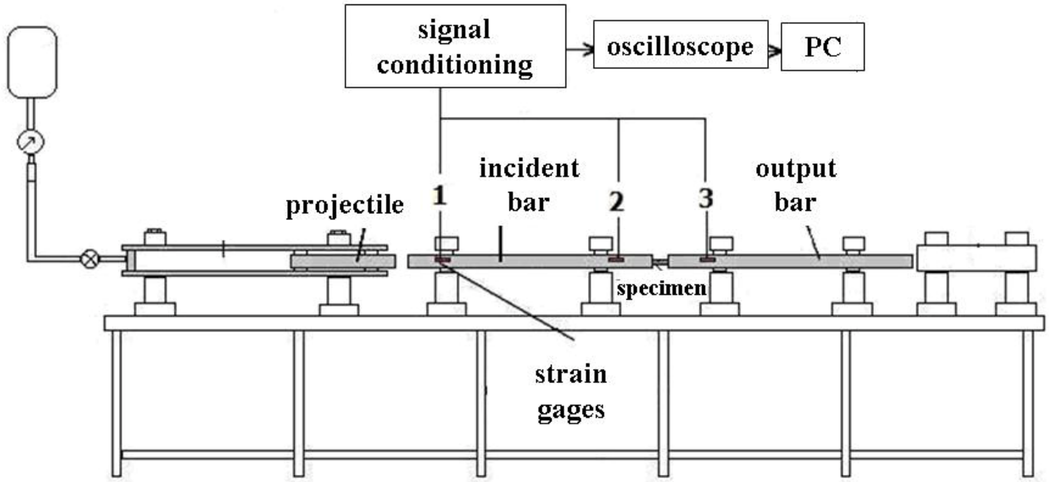

Fig. 1. Schematic representation of the compression Hopkinson Bar setup.

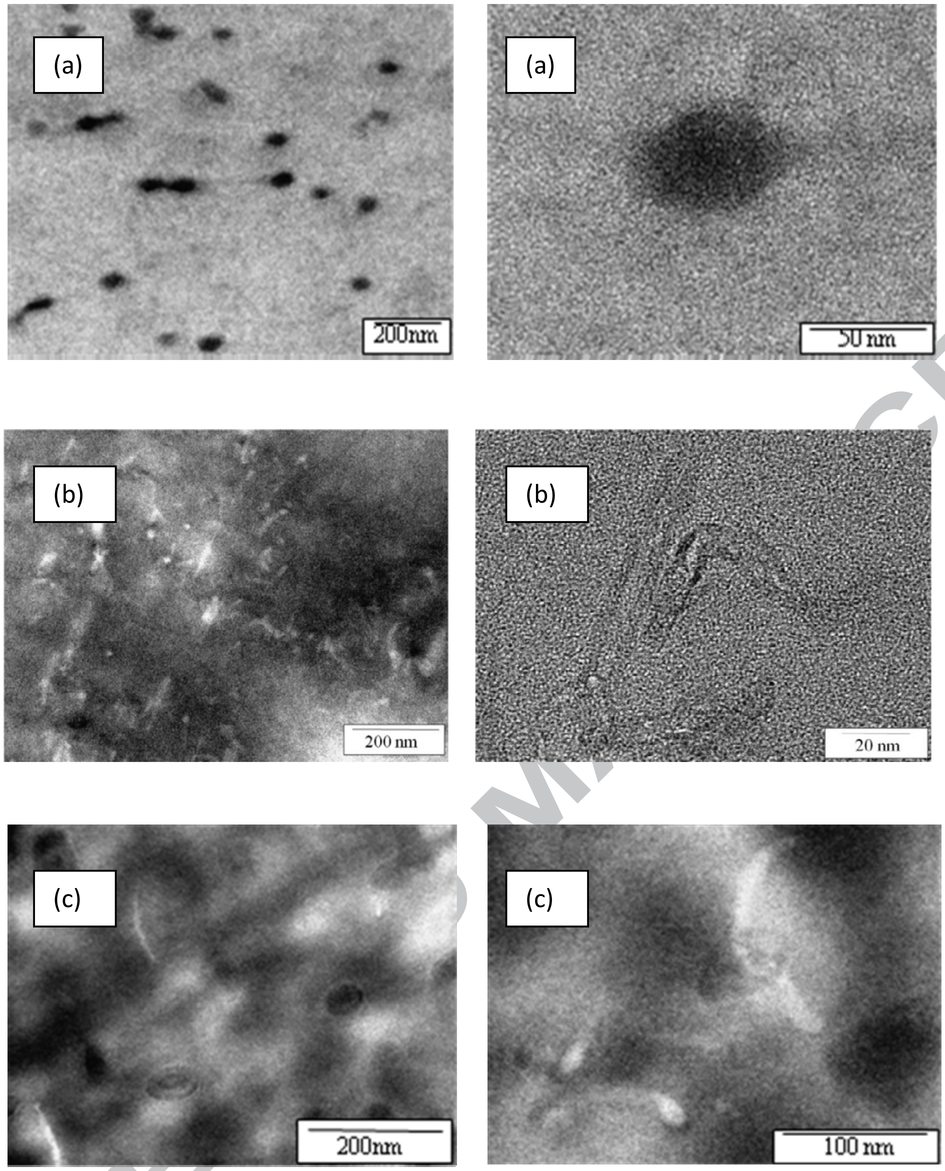

Fig. 2. TEM micrographs of the nanostructured epoxy containing: (a) 5phr SBM triblock copolymer, (b) 0.25 phr CNTs, (c) 5phr SBM triblock copolymer and 0.25phr CNTs.

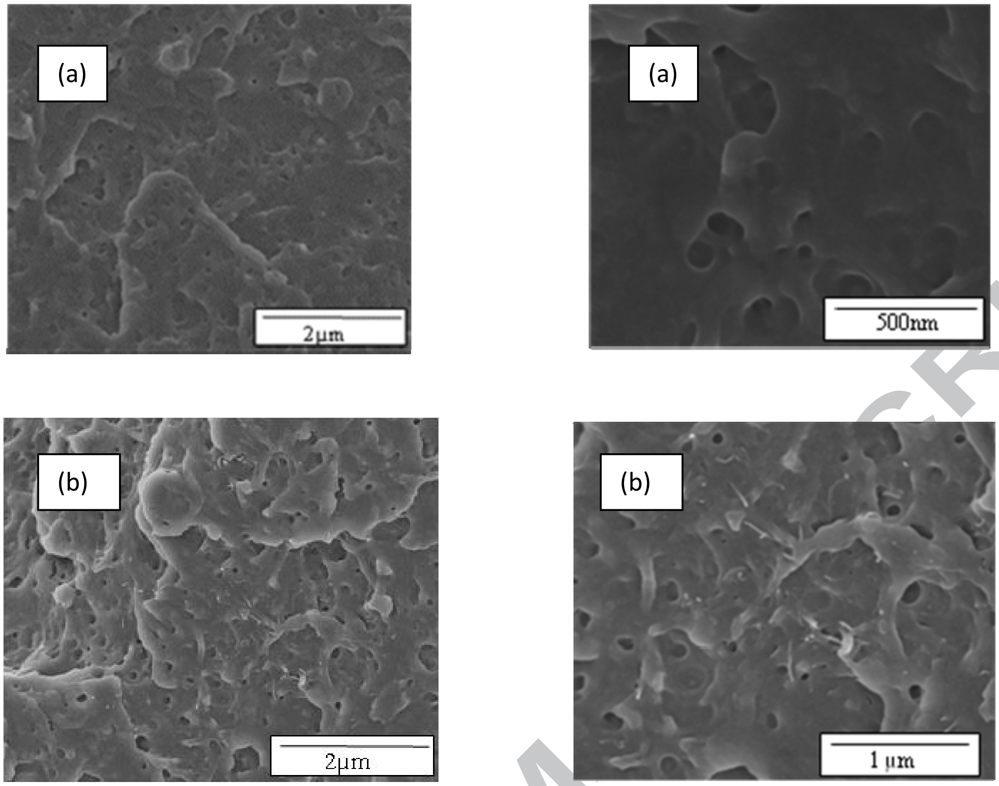

Fig. 3. . FE-SEM micrographs of the fracture surfaces in liquid nitrogen of epoxy containing: (a) 5phr SBM triblock copolymer, (b) 5phr SBM triblock copolymer and 0.25phr CNTs.

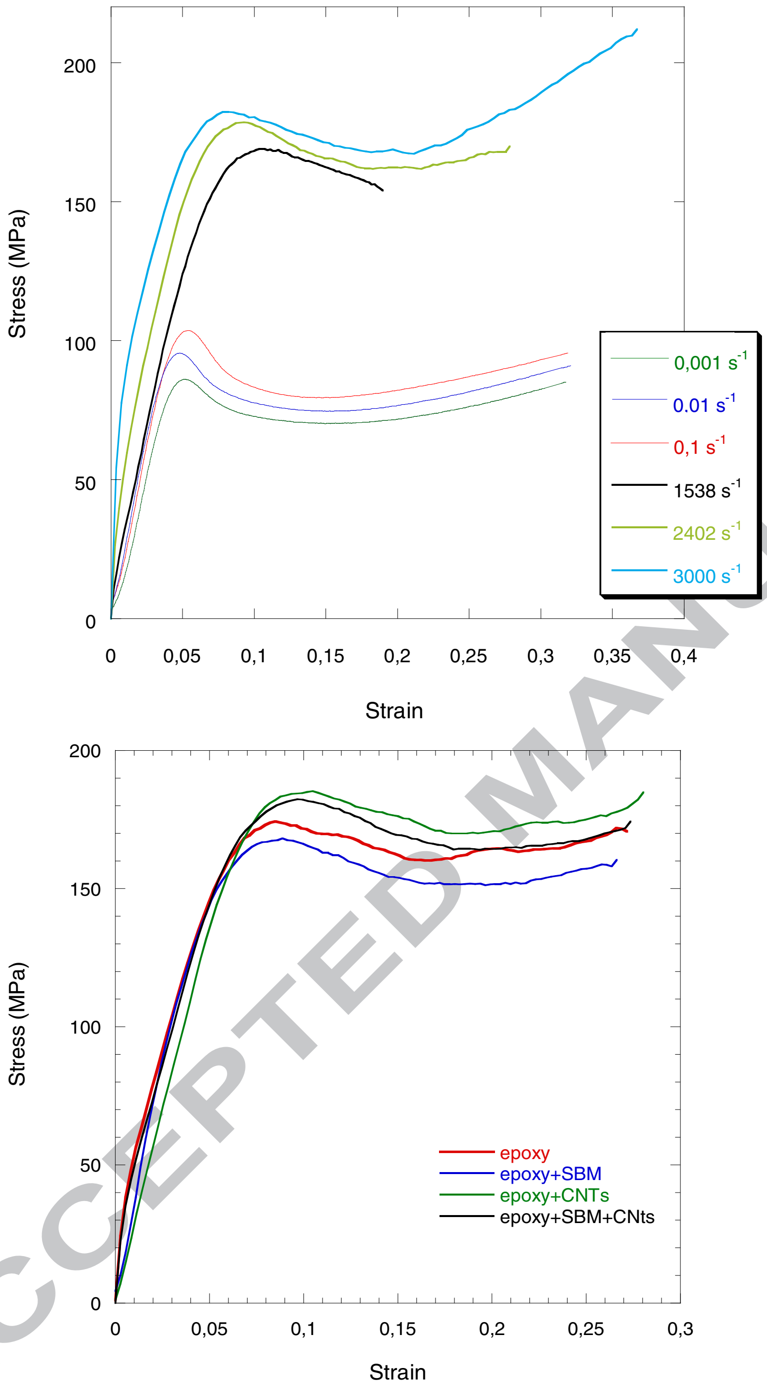

Fig. 4. Stress-strain curves in compression of epoxy carbon nanotubes and SBM triblock hybrid composite at different strain rates (upper graph) and of the four materials studied at 2400 s^{-1} (lower graph).

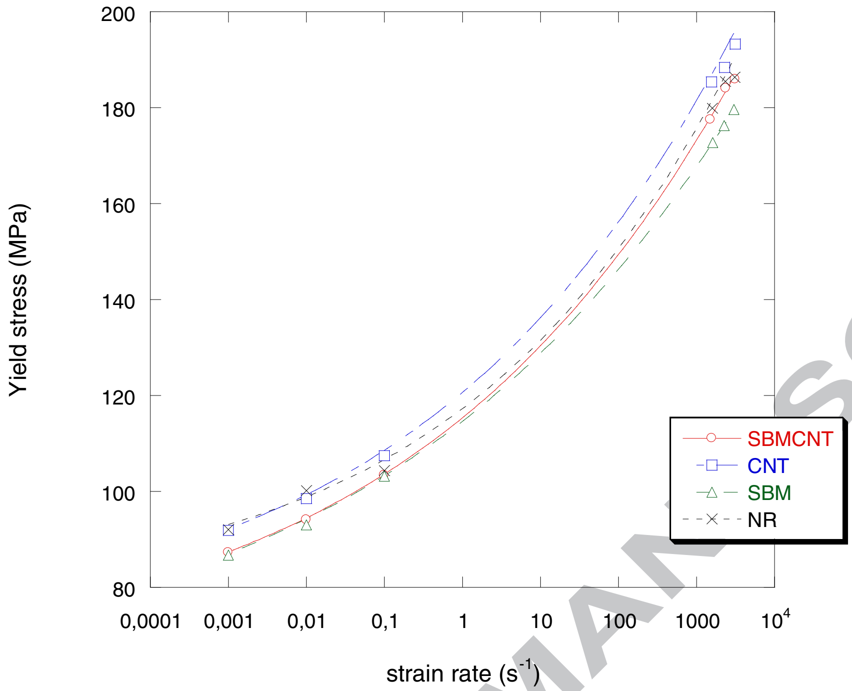

Fig. 5. Compressive yield stress experimental values and its dependence with strain arte for the pure epoxy (NR), SBM modified epoxy (SBM), epoxy reinforced with CNTs (CNT) and hybrid composite with SBM triblock copolymer and CTS (SBM_CNT). The relationship between experimental and numerical values of yield stress calculated using the cooperative model is shown for the four epoxy systems studied.

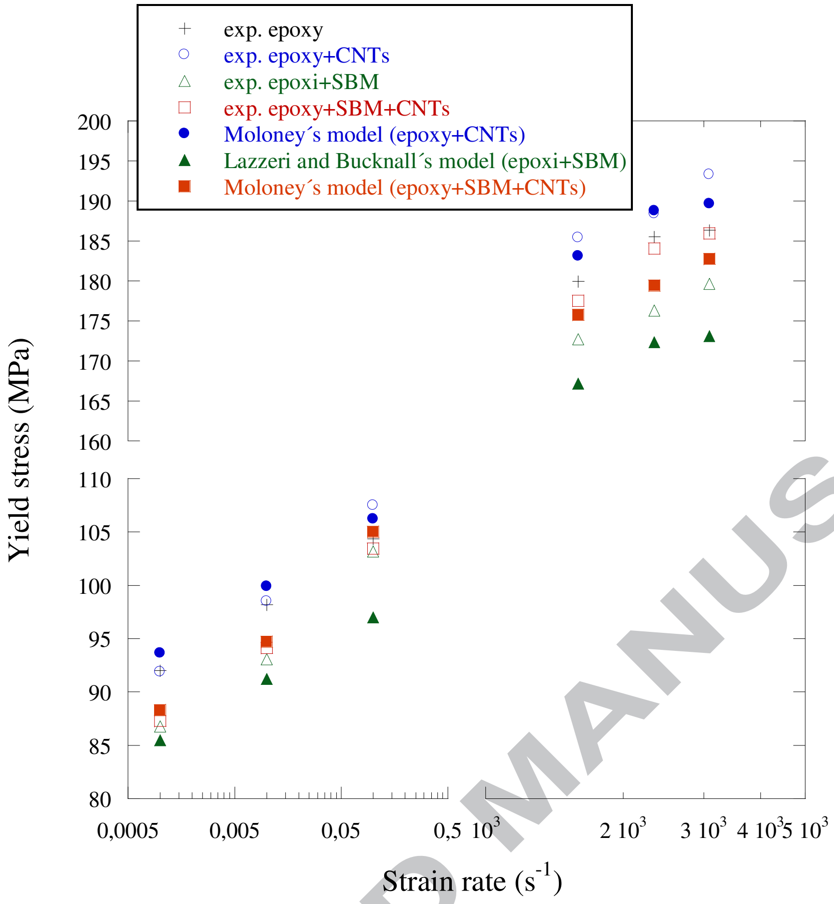

Fig. 6. The relationship between experimental and predicted values of yield stress for the four materials studied.

Table 1. Summary of the Cooperative model parameters for the epoxy systems studied.

Parameter	**Neat epoxy**	**Epoxy+ SBM**	**Epoxy+CNTs**	**Epoxy+ SBM+CNTs**
n	7,44	9,73	8,50	8,91
V (nm^3)	0,039	0,039	0,037	0,037
σ_i (MPa)	77,2	60	69,3	63,2
$\dot{\varepsilon}^{*}$ **(s^{-1})**	$2,51 \cdot 10^{5}$	$6,20 \cdot 10^{5}$	$2,86 \cdot 10^{5}$	$4,63 \cdot 10^{5}$

Table 2. Strain rate sensititvity of epoxy systems under different ranges of strain rate.

Material	**Range of strain rate (s^{-1})**	**Classification**	**Strain rate sensitivity, β (MPa)**
Neat epoxy	0.001-0.1	Quasi-static	2.5
	1570-3200	Dynamic	34
Epoxy+SBM	0.001-0.1	Quasi-static	2.6
	1570-3200	Dynamic	39
Epoxy+CNTs	0.001-0.1	Quasi-static	1.2
	1570-3500	Dynamic	53
Epoxy+SBM+CNTs	0.001-0.1	Quasi-static	2.8
	1570-3400	Dynamic	45